

Mineralogy, Geochemistry, and Age Constraints on the Zn-Pb Skarn Deposit of Maria Cristina, Quebrada Galena, Northern Chile

FRANÇOIS LIEBEN,[†] ROBERT MORITZ, AND LLUÍS FONTBOTÉ

Département de Minéralogie, Université de Genève, rue des maraîchers 13, 1211 Genève 4, Switzerland

Abstract

The Maria Cristina Zn-Pb skarn deposit, hosted by carbonate rocks of the Lower Cretaceous Chañarcillo Group in northern Chile, is described to provide a basis of comparison to adjacent (~2 km) barite deposits and regional Pb-Zn and Ba deposits with Mississippi Valley-type affinities. Strongly retrograded garnet (andradite to $\text{Ad}_{30}\text{Gr}_{70}$), diopsidic pyroxene, and epidote skarn, and barite-bearing massive sulfides (sphalerite-pyrite-galena-marcasite-magnetite) occur at the contact of potassically altered diorite porphyry of mid-Cretaceous age. The skarn mineral compositions, similar to those of Cu skarns, may reflect emplacement in a high f_{O_2} context. Sulfur isotope values of sulfides (–8.8 to +7.1‰) and barite (14.0–26.1‰) indicate disequilibrium conditions and different sulfur sources, including magmatic sulfur. Lead isotope ratios of galena and strontium isotope ratios of barite indicate a similar metal reservoir for the different ore deposit types, constituted by the intercalated Lower Cretaceous volcanic rocks or mid-Cretaceous intrusive rocks. $^{40}\text{Ar}/^{39}\text{Ar}$ dating of hydrothermal K feldspar suggests an age between 94 and 90 Ma for the mineralization.

Introduction

THE MARIA CRISTINA Zn-Pb deposit is located in the Quebrada Galena, about 80 km south of Copiapó and 10 km to the east of the Panamerican highway in northern Chile (Fig. 1). The deposit, of poorly known size, on the order of several 10,000 tons of ore, is hosted by the upper member of the Nantoco Formation. The Nantoco Formation is part of the approximately 1- to 2-km-thick carbonate rocks of the Lower Cretaceous Chañarcillo Group, which were deposited in a back-arc basin setting (Segerstrom, 1968). The Chañarcillo Group is the host of several types of Pb-Zn and Ba ore deposits and occurrences (Lieben et al., 1996; Table 1). These deposits and occurrences include the strata-bound zebra barite lenses of the Mamiña barite belt (Díaz et al., 1981; Díaz, 1990), which are thought to be formed from basin-derived fluids (Lieben et al., 1996, 1999) and are adjacent to the Maria Cristina deposit (Fig. 1). Both the Mamiña barite belt and the Maria Cristina deposit share, in general terms, a similar structural setting and contain barite as a major component. However, the Maria Cristina deposit, and possibly other neighboring ore occurrences, including Carola, Lechuza, and Triunfo (Fig. 1), represent a different mineralization style characterized by their spatial association with potassically altered magmatic rocks and by a high-grade Zn-Pb-rich massive sulfide and a skarn paragenesis. The Maria Cristina deposit and the adjacent ore occurrences belong to the Zn-Pb skarn ore deposit type classically described in the western United States, northern Mexico, and Peru (e.g., Einaudi et al., 1981; Titley, 1993), and which has begun to be recognized within the Chañarcillo Group of northern Chile.

The Maria Cristina deposit is structurally controlled, and occurs at the contact with small altered porphyritic bodies that are related to a Cretaceous hornblende diorite stock (Fig. 1). The aim of this paper is to describe the geology, mineralogy, geochemistry, and isotopic (S, Pb, Sr) systematics of the Maria Cristina deposit, in order to provide a basis for recognition of this ore style in this area, and as a basis of comparison

to the other ore and alteration styles in the Quebrada Galena area, which were described elsewhere. The spatial association of two such different ore styles might be representative of this setting (Lieben et al., 1996; Lieben, 2000). $^{40}\text{Ar}/^{39}\text{Ar}$ ages were obtained for hornblende and K feldspar in order to constrain the timing of intrusion and mineralization.

Geologic Setting

The Lower Cretaceous Chañarcillo Group, which is exposed in a north-northeast-trending belt extending from 27°30' to 29° S across the Atacama region (Fig. 1), forms part of the Andean Mesozoic system of the north-south-oriented arc and back-arc basin developed on a Paleozoic and Triassic basement (Coira et al., 1982; Mpodozis and Ramos, 1989). The Chañarcillo Group consists mainly of shallow marine carbonate rocks (Jurgan, 1977; Cisternas and Díaz, 1990) that overlie and present a lateral facies change to the west with a volcanic arc sequence composed of the calc-alkaline basaltic andesite to dacitic lavas, breccias, volcanoclastic sandstones, and tuffs of the Lower Cretaceous Bandurrias Formation (Segerstrom, 1968; Zentilli, 1974). Magmatism in the Cretaceous arc was in part controlled by north-south crustal-scale faults and progressively migrated eastward, invading the back-arc basin in the mid-Cretaceous (Farrar et al., 1970; Grocott et al., 1994; Ménard, 1995; Dallmeyer et al., 1996). At that time, the marine sedimentation in the back arc ceased and was followed by the deposition of up to 3,000 m of continental clastic and volcanic rocks of the Cerrillos Formation. Both the Chañarcillo Group and the Cerrillos Formation were affected by a Late Cretaceous compressive tectonic phase (Segerstrom, 1968; Arévalo and Grocott, 1997).

The Chañarcillo Group in the Quebrada Galena area is composed of the Nantoco, Totoralillo, and Pabellón Formations (Jurgan, 1977; Abad, 1980; Cisternas and Díaz, 1990; Fig. 1). The Nantoco Formation consists of a lower member with thick-bedded bioclastic and cherty limestones and an upper member with thin-bedded, in part organic-rich, limestones and marls. The Totoralillo Formation consists of thin-bedded limestones, marls, and volcanoclastic sandstones, with

[†] Corresponding author: e-mail, lieben@skynet.be

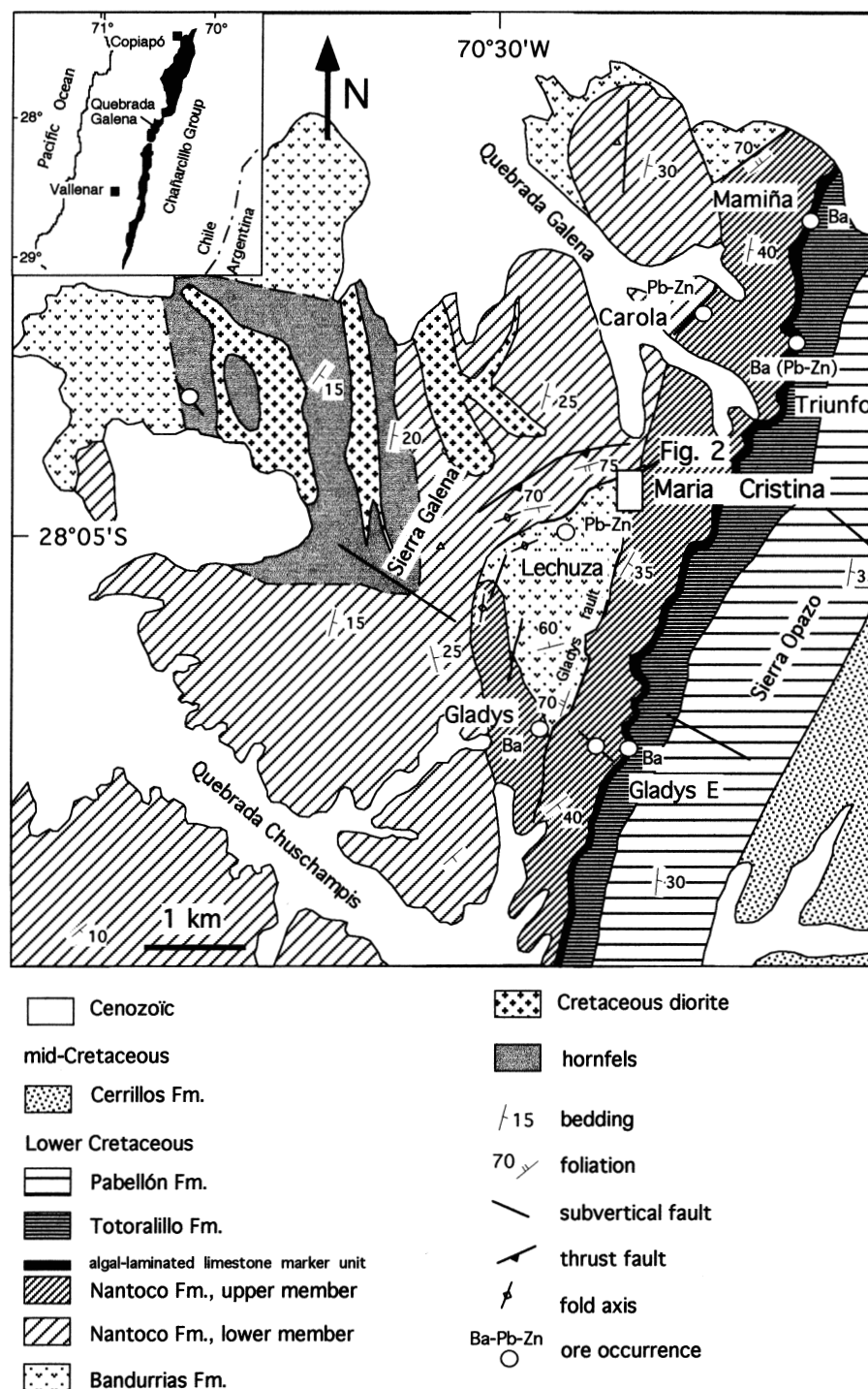


FIG. 1. Geologic map of the Quebrada Galena area, showing the location of the Maria Cristina deposit and the deposits and ore occurrences of the Mamiña barite belt. Geology modified after Abad (1980).

meter-scale bioclastic limestone intercalations. The Pabellón Formation begins with a thick, laterally extensive chert and cherty limestone unit and comprises thick-bedded bioclastic limestones and volcanoclastic sandstones. The sequence composed of the upper member of the Nantoco Formation, the Totoralillo Formation, and the Pabellón Formation might represent a distinct tectonic unit with respect to the lower

member of the Nantoco Formation (Arévalo and Grocott, 1997). A north-northeast-oriented lens south of the Maria Cristina mine, previously defined as a sill (Abad, 1980; Fig. 1), is assigned to the Bandurrias Formation, as it is composed of massive porphyritic lavas of basaltic andesite to dacitic composition, with ≤ 2 mm feldspar and altered mafic phenocrysts in a trachytic, pilotaxitic, or felsitic matrix, which grades into

TABLE 1. Main Characteristics of the Ba and Pb-Zn Occurrence Types Hosted by the Chañarcillo Group

Type	Locality	Paragenesis	Alteration	Fluid inclusions (T_h and salinity)	$\delta^{34}\text{S}$ (‰)	$^{87}\text{Sr}/^{86}\text{Sr}$
Stratiform Pb-Zn-Ba at the base of the Chañarcillo Group	Jaula, Las Cañas tuff-hosted	Gn-Sp-Brt Ag-rich	Chlorite (regional)	70°–150°C (Las Cañas) 6–25 wt % NaCl equiv	Brt, –8 to +17 Gn, –31 to –12	0.7050–0.7055 (Brt)
Stratiform barite in the upper member of the Nantoco Formation	Mamiña belt, Las Cañas barite lens	Brt	Fe-bearing carbonate (Mamiña, Gladys)	70°–150°C (Las Cañas) 150°–250°C (Mamiña) 10–25 wt % NaCl equiv	Brt, 15 to 21	0.7050–0.7066 (Brt)
Vein-type Ba (in part related to Ag districts) and Pb-Zn	Las Cañas, Quebrada Galena Quebrada Chañarcillo	Gn-(Sp) Cu-Ag-rich	Fe chlorite (Las Cañas)	100°–160°C (LC type I) 3–12 wt % NaCl equiv 100°–120°C (LC type II) 26–40 wt % NaCl equiv	Brt, 11 to 14 (Chañarcillo) Gn, –12 (Las Cañas)	0.7038–0.7050 (Brt)
Zn-Pb-(Ba) skarn	Maria Cristina	Sp-Py-Gn- (Mc-Mag)	Skarn, marble potassic alteration	250°–400°C (garnet)	Brt 14 to 26 Sulfides, –9 to +7	0.7048–0.7059 (Brt)

Mineral abbreviations: Brt = barite, Gn = galena, Mag = magnetite, Mc = marcasite, Py = pyrite, Sp = sphalerite

lava breccias, as well as abundant volcanoclastic rocks and bioclastic limestone intercalations.

Cretaceous diorite and quartz diorite subvertical north-northwest-oriented sheets about 100 m thick intrude the Bandurrias Formation and the lower part of the Chañarcillo Group in the area to the north and west of the Sierra Galena (Abad, 1980; Fig. 1). The rocks of this intrusive stock present a variable medium-grained equigranular (0.1–1 mm) to porphyritic texture, with phenocrysts up to 1 cm, and are composed of amphibole and/or pyroxene phenocrysts, zoned plagioclase phenocrysts, in a locally quartz-bearing matrix. In places, the stock is surrounded by a metamorphic halo meters to hundreds of meters wide, consisting of meta-andesites and epidote-garnet-diopside hornfels, and subordinate quartzites and marbles (Abad, 1980; Fig. 1). The magmatic sheets extend to the east to upper stratigraphic levels in the form of smaller discordant and concordant diorite bodies, including the Maria Cristina porphyry and dacite bodies. Basic dikes and sills of meter size, abundant in the upper levels of the Nantoco Formation, are explained, in accordance with Segerstrom (1968) and Tilling (1976) in the Copiapó area, as lamprophyre related to the Cretaceous granitoids which they crosscut.

Structural and Lithological Control of the Ore Occurrences in the Quebrada Galena Area

The Maria Cristina deposit is hosted by a folded and thrust faulted rock sequence above a basal thrust fault that is exposed in the Sierra Galena (Fig. 1). Northwest-directed thrusting and folding is interpreted as resulting from the Late Cretaceous tectonic phase (Lieben, 2000). The Maria Cristina deposit occurs in the folded sequence at the intersection between two major northeast- and north-northeast-striking faults observable on the satellite image (Díaz et al., 1981; Fig. 1). These subvertical to east-dipping faults have younger rocks on their eastern sides, indicating a resultant normal displacement. The north-northeast-striking fault is an extension of the subvertical fault which controls the barite

lens at Gladys. It has not been directly observed at Maria Cristina, where it is apparently a lower angle fault separating the north-northeast-oriented lens of folded rocks of the Bandurrias Formation to the west from relatively flat-lying thin-bedded limestone of the upper member of the Nantoco Formation to the east (Fig. 2). The northeast-trending fault brings rocks of the Bandurrias Formation above thick-bedded limestones of the lower member of the Nantoco Formation. Ore occurrences are also located at the faulted contact between the lower and upper members of the Nantoco Formation at Carola and Lechuza, situated to the north and to the southwest of the Maria Cristina mine, respectively (Fig. 1). The other ore occurrences that belong to the Mamiña belt are at a higher stratigraphic level and are lithologically controlled by a laterally extensive 10-m-thick algal-laminated limestone and stratiform breccia unit (Díaz, 1990; Lieben, 2000; Fig. 1). The main barite lens in the Mamiña mine is up to 2.5 m thick, 100 m in width, and 600 m long and extends along strike discontinuously up to the Triunfo mine about 1.5 km to the south, where barite occurs with a higher Pb and Zn content at the contact of a lamprophyric sill. A coarse- to very coarse grained (1–3 mm) Mg- and Fe-bearing euhedral calcite cement, which overprints the original algal lamination, occurs in spatial association with the barite lenses. According to fluid inclusion data on barite, the mineralizing fluids had temperatures higher than 150° to 250°C and salinities in the range of 9 to 25 wt percent NaCl equiv.

The Zn-Pb Skarn Deposit of Maria Cristina

Geology of the mine area

A surface geologic map of the Maria Cristina mine area and a lithologic column of the mine sequence are shown in Figures 2 and 3, respectively. The exploited orebody is almost entirely hosted by the fault-bound sequence with a dominantly volcanic to volcanoclastic nature below the inferred low-angle north-northeast-striking fault. This sequence is affected by folding and shearing and comprises greenish fossiliferous

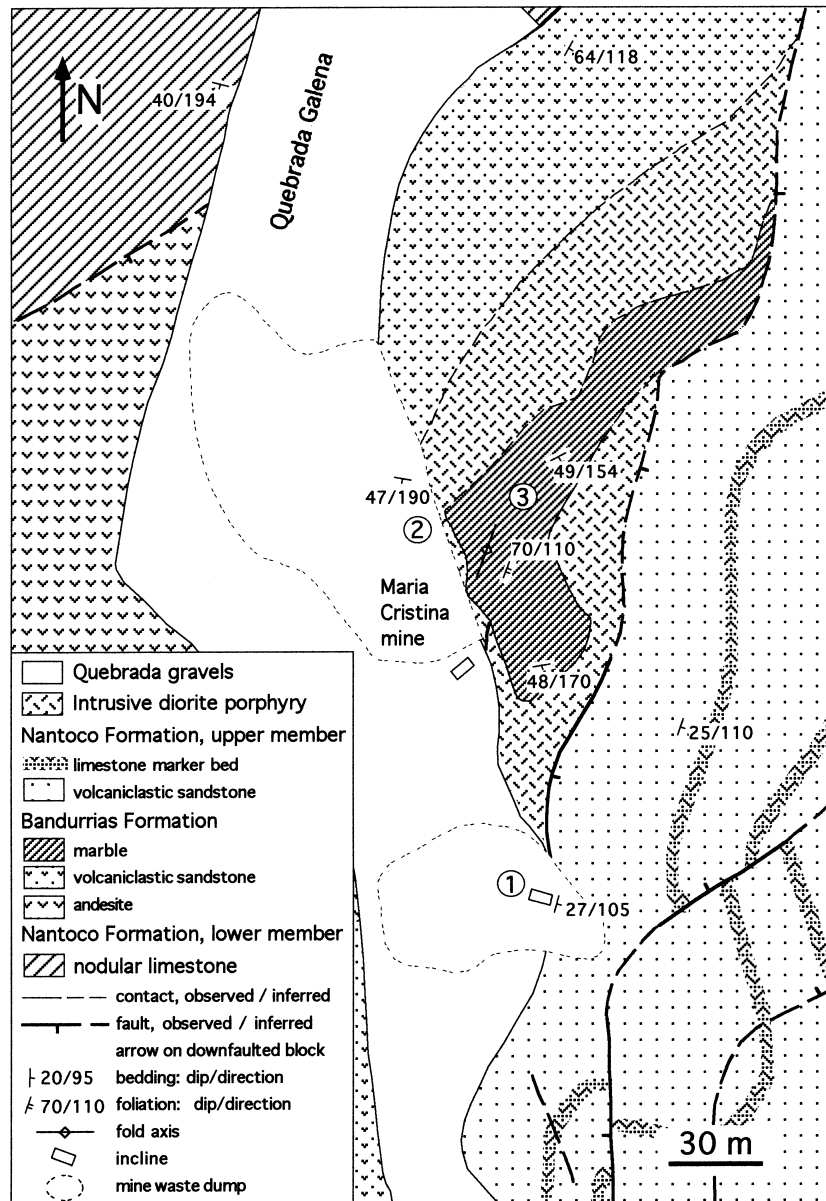


FIG. 2. Geologic map of the Maria Cristina mine. The circled numbers correspond to old workings areas referred to in the text.

calcareous sandstone, mudstone, breccia, and tuff, as well as meter-scale beds and lenses of white marble and ankeritic marble, which are at the immediate contact of the partly concordant intrusive hornblende diorite porphyritic bodies (Fig. 3). To the west of the mine, the fault-bound sequence is dominated by massive and brecciated andesitic lavas (Fig. 2). The overlying sequence of the upper member of the Nantoco Formation is composed of micritic limestone, bioclastic limestone, and well-sorted medium- to fine-grained volcaniclastic rocks (Fig. 3).

Old workings follow the upper concordant contact of the porphyry (area 1, Fig. 2), a discordant contact down to more than a 75-m depth (Schwarze, 1946; area 2, Fig. 2), and a barite-rich orebody within ankeritic marble cut by intrusive bodies tens of centimeters across (area 3, Fig. 2). Potassic and

sericitic alteration affects a large part of the porphyry. A coarsely crystalline garnet, pyroxene, and epidote skarn, strongly affected by retrograde alteration, forms lenses tens of centimeters to meters thick at the intrusion-limestone contact. The sulfides occur as massive replacement bodies meters to tens of meters across (Schwarze, 1946). The sequence of alteration within the carbonate rock and of the mineralization includes a prograde skarn stage, followed by a retrograde and sulfide stage.

Alteration of the intrusion

The least altered equivalent of the porphyritic intrusion at Maria Cristina shows propylitic alteration, marked by strong chloritization of amphibole phenocrysts and sericitization of plagioclase phenocrysts, and by the development of calcite,

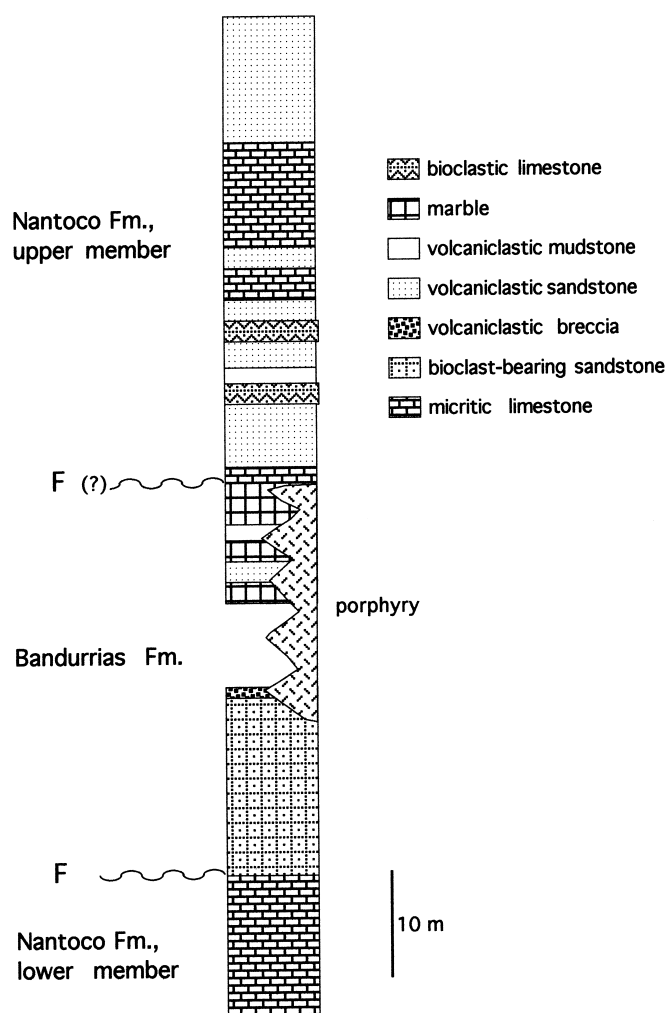


FIG. 3. Schematic lithologic column of the Maria Cristina mine sequence on the eastern side of the Quebrada Galena.

quartz, and pyrite in the matrix. Local sericitic alteration of the intrusion is characterized by the complete replacement of plagioclase phenocrysts by 100- to 200- μ size sericite crystals, amphibole phenocrysts by chlorite, as well as the leaching of sulfides. Abundant smectite in the sericitically altered rock, together with the leaching of sulfides, may reflect the supergene alteration of the orebody.

Potassic (K feldspar) alteration affecting the intrusion is relatively strong, resulting in over 7 wt percent K_2O in the altered rock (Fig. 4), and occurs notably at the contact with skarn bodies. A weaker potassic alteration halo, expressed by K feldspar and sericite, and locally sodic alteration, affects the volcanic and volcaniclastic rocks of the north-northeast lens of the Bandurrias Formation around the ore deposit (Fig. 4). Tuffs and tuffaceous limestones that enclose the mineralized lens at the Triunfo ore occurrence also present a high K_2O content, probably also due to potassic alteration (Fig. 4). The potassic alteration assemblage in the Maria Cristina mine is composed of pink to white potassic feldspar (K feldspar \gg plagioclase), quartz, and chlorite, with some sericite, tourmaline, and apatite, and is fabric destructive. This assemblage is in part overprinted by large carbonate and pyrite crystals.

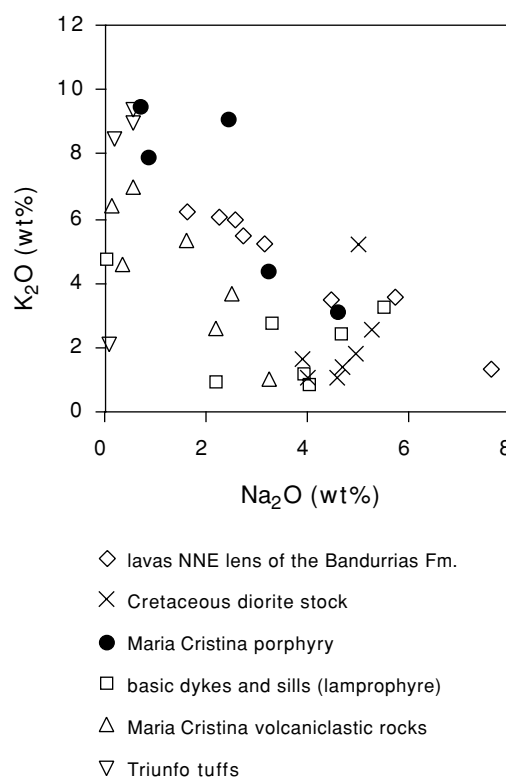


FIG. 4. Na_2O vs. K_2O diagram of magmatic rocks from the Quebrada Galena area. The lava samples of the north-northeast lens of the Bandurrias Formation show a negative correlation interpreted as the result of alkali metasomatism. A strong potassic alteration ($K_2O > 7\%$), expressed by K feldspar, affects parts of the Maria Cristina porphyry and some volcaniclastic rocks in the Triunfo mine. Copper mineralization in the Copiapó area is commonly spatially related to such potassic alteration (Marschik, 1996).

Alteration of the carbonate host rock

The alteration of the carbonate host rock at Maria Cristina is marked by the recrystallization of the limestone to marble and by the formation of coarsely crystalline skarn lenses due to the ingress of Si-, Al-, Fe-, and Mg-rich fluids in the host rock. The prograde skarn mineral assemblage comprises garnet, clinopyroxene, magnetite, and epidote. The presence of former pyrrhotite is evidenced by its pseudomorphic replacement by marcasite, pyrite and calcite (Blätterteiggefüge, see Ramdohr, 1980). The garnet consists of anisotropic and isotropic zoned andradite to $Ad_{30}-Gr_{70}$, with a mean spessartine and almandine content approaching 10 mole percent for the grossular end member (Figs. 5A and 6). Its composition is close to those of garnets from Zn-Pb skarns (Einaudi et al., 1981; Meinert, 1992). Anisotropic zones, including 1-mm cores of the crystals, tend to be more aluminum rich and yield a higher Ti content than the isotropic andraditic overgrowth. By comparison, garnet within tuffaceous limestone from Triunfo also shows Ti-rich core but is closer to grossular compositions, suggesting an origin through reaction (reaction skarn). Relicts of millimeter-long clinopyroxene from Maria Cristina consist principally of diopside with less than 10 mole percent hedenbergite (Fig. 6). Unlike typical pyroxenes from Zn-Pb skarns (Meinert, 1987), there is no Mn enrichment at Maria Cristina. The pyroxene of this study is more like those of Cu

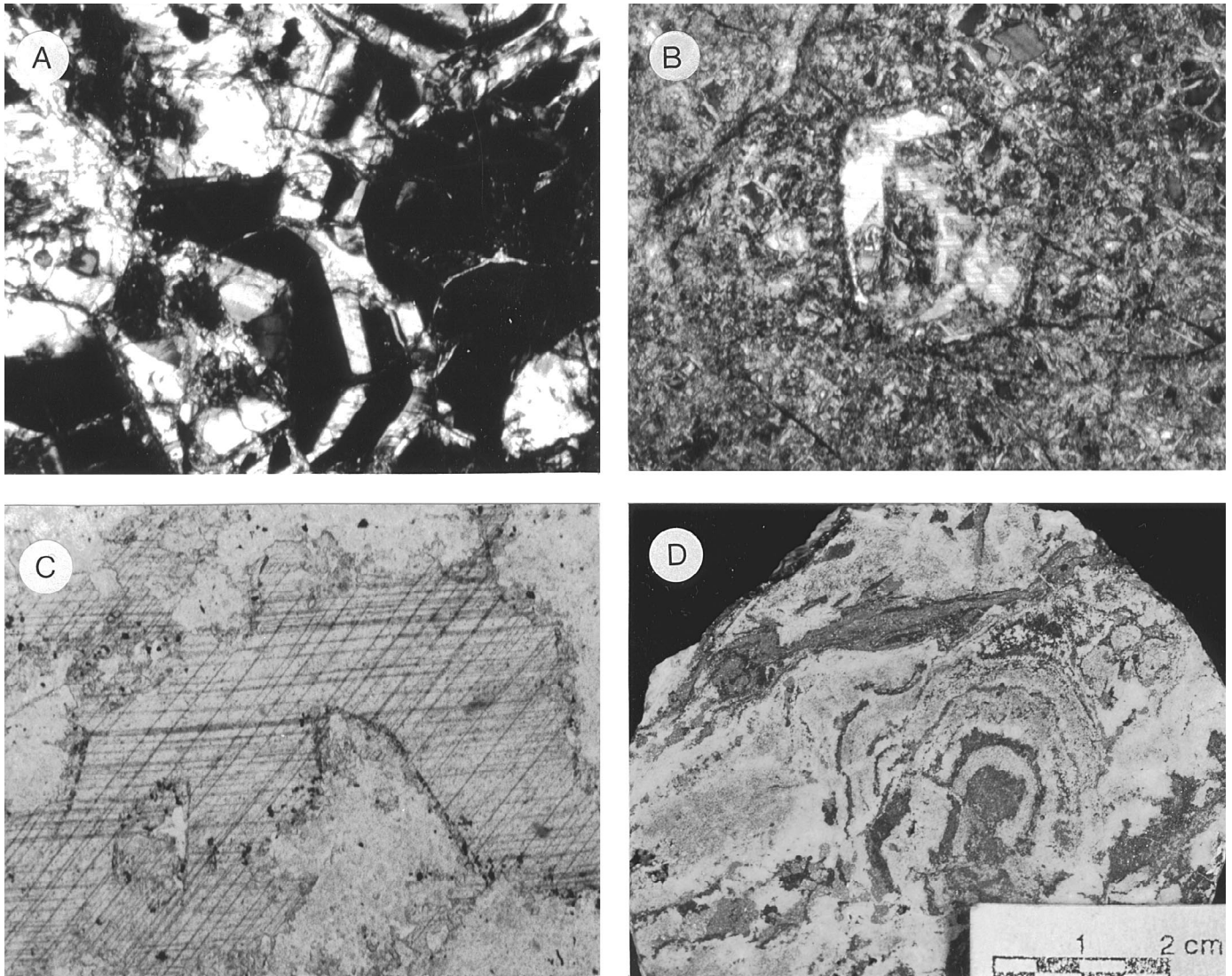


FIG. 5. Skarn and sulfide assemblages. A. Zoned garnet of andradite to $Ad_{30}-Gr_{70}$ composition. B. Pseudomorphous replacement of garnet by chlorite, calcite and quartz. C. Retrograde assemblage of albite, quartz, chlorite, sericite, calcite, and pyrite, with coarse-grained epidote relicts. All photomicrographs with transmitted light, field of view is 3 mm D. Finely banded sulfide (sphalerite-galena-pyrite) ore in calcite and barite gangue.

skarns, which may reflect higher f_{O_2} conditions (Einaudi and Burt, 1982). The pyroxene skarn is usually strongly altered to an assemblage dominated by carbonate and talc, whereas chlorite, calcite, quartz, and clay-rich assemblages may be largely pseudomorphous after garnet skarn (Fig. 5B). The coarse-grained epidote is relatively well preserved but occurs as relicts in an albite-rich assemblage (Fig. 5C).

Mineralization

The mineralization consists of coarse-grained pyrite-rich massive sulfides within the carbonate host rock and massive to semimassive sulfides in the retrograde skarn and within the matrix of the coarse-grained volcanoclastic host rocks. A compositional banding is generally visible, ranging from a broad millimeter-scale banding to a delicate banding of metasomatic origin (Fig. 5D), and textures of primary prograde skarn minerals are locally preserved in skarn-hosted ores.

Veinlets and disseminated pyrite and sphalerite occur in the altered magmatic rocks. The ore minerals comprise sphalerite, pyrite, and galena, lesser marcasite and magnetite, and trace amounts of chalcopryrite and tetrahedrite, notably as inclusions in galena. The magnetite tends to occur, notably in skarn-hosted ores, in galena-poor, Fe-rich sphalerite and pyrite seams, whereas the marcasite is mainly found as rims between sulfides and a late carbonate in association with Fe-poor sphalerite, galena, and barite in the more distal sedimentary rocks (Fig. 7). The sulfides are commonly intergrown with retrograde minerals of the skarn, including chlorite, talc, quartz, calcite, and clays, along with barite (Fig. 7).

Barite is an abundant gangue mineral, which occurs notably as a late phase associated with the distal sulfides. Baritic lenses in the marble outcrop (area 3, Fig. 2) consist of veinlets and irregular barite bodies with various amounts of clays

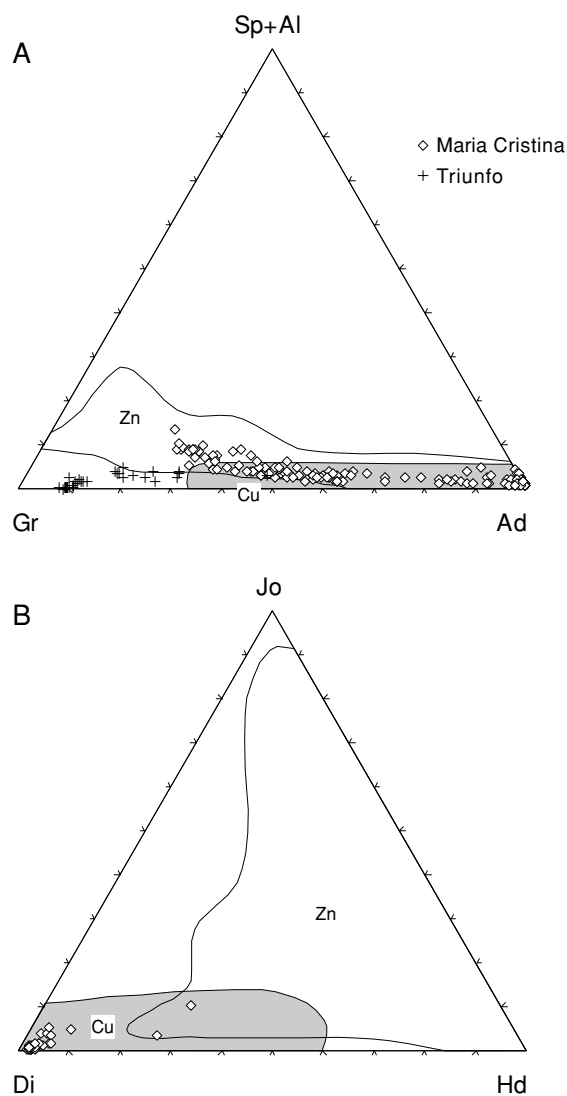


FIG. 6. A. Analyses of garnets from the Maria Cristina skarn and from Triunfo (reaction skarn?) in the spessartine + almandine-grossular-andradite system. B. Analyses of clinopyroxenes from the Maria Cristina skarn in the johannsenite-diopside-hedenbergite system. Fields of typical garnets and pyroxenes from Pb-Zn and Cu skarns indicated with a solid line, after Meinert (1992).

and oxidized Pb and Zn minerals. The massive sulfides and sulfide barite ores have been partly affected by later deformation and are cut by numerous quartz and calcite veinlets.

The skarn, massive sulfide, and volcanoclastic-hosted ores are characterized by a high Fe, Zn, and Pb content, relatively high Mn, a strongly subordinate Cu content, and a high Zn/Pb ratio (≥ 4 , Table 2) in line with typical Zn-Pb skarns (Einaudi et al., 1981). Consistent with the mineralogical trend, the Fe content and Zn/Pb ratio decrease from skarn to massive sulfide and volcanoclastic-hosted ores. The mean Ag content is also relatively high, which is common in Zn-Pb skarns (Titley, 1993). Higher Ag concentrations, along with As and Sb, occur in galena-rich samples. The gold content ranges up to 0.16 ppm (Table 2).

TABLE 2. Geochemical Analyses of Sulfide and Barite Ores from Maria Cristina and Carola

Locality	Sample no.	Description	Fe (%)	Ba (ppm)	Mn (ppm)	Cu (ppm)	Pb (ppm)	Zn (ppm)	Ag (ppm)	As (ppm)	Sb (ppm)	Cd (ppm)	Au (ppb)	Hg (ppm)	Zn/Pb
Maria Cristina	327B-1	Massive Py-Sp-Gn ore	12.9	110	3,986	1,533	31,885	175,000	271	200	77	834	<2	18	5.5
Maria Cristina	326B-6	Massive Py-Sp in retrograde skarn	16.7	750	2,763	1,266	781	179,000	4	37	4.4	515	53	6	229.2
Maria Cristina	326B-9	Replacement Py-Sp-Gn with Cal and Brt	7.11	30,000	7,568	304	35,178	155,000	32	120	18	522	158	12	4.4
Maria Cristina	326B-10	Py-Mc-Sp-Gn-Cal in volcanic breccia	12.9	2,200	5,768	253	11,246	54,973	42	2,100	75	188	7	<1	4.9
Maria Cristina	326-1A	Massive Py-Sp in retrograde skarn	20.6	1,500	n.a.	n.a.	n.a.	116,800	<5	73	15	n.a.	120	<1	
Maria Cristina	346	Massive Sp-Gn-Py ore	4.22	26,000	n.a.	n.a.	n.a.	221,800	470	410	290	n.a.	3	8	
Carola	339-4	Massive Sp-Gn-Py-Mc ore	12	480	n.a.	n.a.	n.a.	220,700	48	1,300	160	n.a.	3	28	
Maria Cristina	327B-4	Bluish barite replacement ore	0.51	340,000	312	40	1,747	10,719	11	44	6	251	<2	<1	6.1
Maria Cristina	88	Brecciated barite in oxidized ore	4.83	170,000	1,571	170	17,197	4,517	8	1,600	120	4	<4	<1	0.3
Carola	344-1	Brecciated barite in oxidized ore	21.9	75,000	2,286	154	859	10,015	3	1,700	210	<0.5	13	<1	11.7

Analyses made by ICP and INAA at Actlabs, Canada

Abbreviations: Brt = barite, Cal = calcite, Gn = galena, Mc = marcasite, Py = pyrite, Sp = sphalerite; n.a. = not available

	prograde	retrograde and ore stage	
		proximal	distal
garnet (Ad-Gr)			
epidote			
pyroxene (Di)			
K-feldspar			
albite			
tourmaline (tr.)			
apatite (tr.)			
quartz			
calcite			
chlorite			
talc			
sericite			
sphalerite		black sp	cream sp
galena			
pyrite			
pyrrhotite			
magnetite			
marcasite			
hematite (traces)			
chalcopryite (traces)			
tetrahedrite (traces)			
barite			

FIG. 7. Paragenetic sequence of the skarn, massive sulfide, and volcani-clastic-hosted ores at Maria Cristina.

Isotopic Studies

Sulfur isotope analyses of sulfides and barite, strontium isotope analyses of barite, and lead isotope analyses of galena were carried out on optically pure mineral separates from the Maria Cristina deposit and from the various Ba and Pb-Zn ore

deposit types within the Chañarcillo Group. The analytical methods and results are reported in Lieben et al. (1996, 1999). Additional sulfur isotope analyses of sulfide and barite from Maria Cristina (Table 3) were performed on SO₂ produced by the combustion with tungsten oxide on a Finnigan MAT 251 mass spectrometer at the University of Lausanne. Previous sulfur isotope data of galenas and barite are also given by Spiro and Puig (1988).

The lead isotope ratios of four galena samples of volcani-clastic-hosted and massive sulfide ores from Maria Cristina and a cerussite sample from Triunfo are relatively homogeneous and are similar to those of the Lower Cretaceous-hosted strata-bound deposits of northern and central Chile (Puig, 1988; Lieben et al., 1999). The lead isotope data for Maria Cristina suggest that the Lower Cretaceous volcanic and volcani-clastic host-rock sequence, which is viewed as a major source of metals for the strata-bound deposits (Puig, 1988; Lieben et al., 1999), might have provided the lead for the mineralization. However, because of probable partial overlap between lead isotope signatures of Lower Cretaceous volcanic rocks and Cretaceous intrusive rocks (Marschik et al., 1997), and in the absence of data for local sources, we cannot exclude that part or most of the lead was derived from the dioritic intrusion.

The strontium isotope composition of barites from Maria Cristina, ranging from 0.7048 to 0.7059, indicates mixing between an Sr-rich source with low-radiogenic Sr and an Sr-depleted source with a seawater Sr isotope signature (Lieben et al., 1996). The low-radiogenic Sr source is most likely the volcanic rocks of the Bandurrias Formation or the Cretaceous intrusive rocks, whereas the more radiogenic source corresponds to the carbonate host rock (Lieben et al., 1996). Barites from the Mamiña belt present relatively high strontium

TABLE 3. Isotopic Data from the Maria Cristina Pb-Zn Deposit

Sample no.	Mineral	$\delta^{34}\text{S}$	$^{87}\text{Sr}/^{86}\text{Sr}$	Sr (ppm)	$^{206}\text{Pb}/^{204}\text{Pb}$	$^{207}\text{Pb}/^{204}\text{Pb}$	$^{208}\text{Pb}/^{204}\text{Pb}$	Description
FX-326B-5	Pyrite	-6.0						Massive Py with Mt and Cal
FX-326B-6	Pyrite	29.3						Massive Py-Sp in retrograde skarn (black Sp)
FX-326B-6	Sphalerite	-8.8						Replacement Py-Sp-Gn ore (black Sp)
FX-326B-9	Sphalerite	-3.0						Replacement Py-Sp-Gn ore (brown Sp)
FX-326B-9	Sphalerite	-5.8						Replacement Py-Sp-Gn ore
FX-326B-9	Galena				18.406	15.560	38.158	Replacement Py-Sp-Gn ore
FX-326B-9	Barite	17.5						Replacement Py-Sp-Gn ore
FX-326B-10	Py-Mc	7.1						Py-Mc-Sp-Gn-Cal in volcanic breccia
FX-326B-10	Galena	1.0			18.450	15.616	38.337	Py-Mc-Sp-Gn-Cal in volcanic breccia
FX-327B-2	Galena	-2.6			18.408	15.564	38.165	Py-Mc-Sp-Gn-Cal in volcanic breccia
FX-327B-6	Sphalerite	4.0						Sp-Gn-Brt in lapilli tuff (cream Sp)
FX-327B-6	Galena	-6.4			18.443	15.612	38.325	Sp-Gn-Brt in lapilli tuff
FX-327B-6	Barite	17.6						Sp-Gn-Brt in lapilli tuff
FX-394-7	Barite	24.8						Sp-Gn-Brt in lapilli tuff
FX-326-3	Barite	20.5	0.70515	4477				Massive Sp-Gn-Py and barite
FX-346	Barite	21.6	0.70594	3047				Massive Sp-Gn-Py and barite
FX-085	Barite	17.07 ¹	0.70478	7115				Barite in oxidized ore
FX-088	Barite	26.08 ¹	0.70563	5109				Brecciated barite in oxidized ore
FX-086	Barite	16.69 ¹						Barite band in ankeritic marble
FX-087	Barite	17.54 ¹						Barite band in ankeritic marble
FX-326-5	Barite	15.3	0.70499	5331				Barite in sulfide-bearing marble
FX-395-4	Barite	14.0						Barite in white marble
FX-309	Barite	16.4 ¹	0.70481	6105				Barite vein in andesite
FX-103 (Triunfo)	Cerussite				18.433	15.595	38.275	Oxidized ore

¹ Sulfur isotope analyses previously reported in Lieben et al. (1996)

Abbreviations: Brt = barite, Cal = calcite, Gn = galena, Mc = marcasite, Mt = magnetite, Py = pyrite, Sp = sphalerite

isotope ratios, in the range 0.7053 to 0.7066, but still lower than the Lower Cretaceous seawater ratio, indicating an input of strontium from the leaching of volcanic or intrusive rocks.

The $\delta^{34}\text{S}$ values of nine sulfide samples from the Maria Cristina deposit range from -8.8 to $+7.1$ per mil, with an anomalous value of 29.3 per mil for one pyrite sample. The $\delta^{34}\text{S}$ values of 12 barite samples from Maria Cristina range from 14.0 to 26.1 per mil, which represents a larger spread than the $\delta^{34}\text{S}$ range of barites from the Mamiña barite belt (Fig. 8; Table 3). Among sulfides, pyrite presents the widest range in sulfur isotope composition (-6.0 to $+29.3\text{‰}$), followed by sphalerite (-8.8 to $+4.0\text{‰}$), and galena (-6.4 to $+1.0\text{‰}$). Sulfides from the relatively distal low iron paragenesis hosted by the coarse-grained volcanoclastic rocks tend to display higher $\delta^{34}\text{S}$ values (mean 1‰) than the other sulfides (mean -6‰ , excluding the anomalous pyrite). Distal barites with few associated sulfides tend to cluster, together with barites from the Mamiña barite belt, around Lower Cretaceous seawater sulfate value (around 16‰), whereas some barites that are intergrown with significant amounts of sulfides show higher $\delta^{34}\text{S}$ values (Table 3).

Pairs of coexisting sulfide minerals yield elevated $\Delta^{34}\text{S}$ values, giving a sulfur isotope fractionation temperature of $136^\circ \pm 16^\circ\text{C}$, according to the equation of Ohmoto and Rye (1979), for a pyrite and marcasite-galena pair hosted by volcanic breccia and two negative temperatures, respectively, for a pyrite-sphalerite pair involving the anomalous value of 29.3 per mil, and for a sphalerite-galena pair. Two sulfide barite pairs yield fractionation temperatures of 263° to 312°C and 289° to 535°C , respectively, depending on which sulfide is chosen for the calculation. The fact that one sphalerite gives anomalous $\Delta^{34}\text{S}$ values with galena and barite may indicate that it was contaminated by the barite. Alternatively, the incoherent calculated sulfur isotope fractionation temperatures may indicate a disequilibrium between the sulfur species, i.e., either that adjacent minerals were not deposited contemporaneously or that a true disequilibrium state existed between the sulfur species during ore minerals precipitation (Ohmoto and Rye, 1979). This is further supported by the fact that the sulfur isotope values for galena, sphalerite, and pyrite samples are not following a normal order of $\delta^{34}\text{S}$ enrichment for these minerals.

The sulfur isotope values of sulfides around 0 per mil were interpreted by Spiro and Puig (1988) to indicate a magmatic source of the sulfur. The relatively large range of $\delta^{34}\text{S}$ values

in this study (Fig. 8; Table 3), however, suggest there are different sources or different mechanisms affecting the sulfur species from such a magmatic source. The higher $\delta^{34}\text{S}$ values in distal sediment-hosted sulfides may indicate a marine sulfate input or alternatively either a transition from oxidizing to reduced conditions or a pH increase of the fluids (Rye and Ohmoto, 1974). Similarly, a diverse origin of sulfur for the barites is supported by a wider spread in $\delta^{34}\text{S}$ values shown by the barites of Maria Cristina relative to the $\delta^{34}\text{S}$ range of barites from the Mamiña barite belt (Fig. 8). The data may support a mixing of seawater-derived sulfate, involved in the more distal barites of Maria Cristina and barites from the Mamiña barite belt, and sulfate derived from the hypogene oxidation of magmatic sulfide, which would be present only in the Maria Cristina deposit.

$^{40}\text{Ar}/^{39}\text{Ar}$ Dating

Sampling and analytical methods

Two samples were dated: the first is a hornblende from the main intrusive body west of the Sierra Galena ($28^\circ 04' 50'' \text{S}$, $70^\circ 30' 50'' \text{W}$), the second is a potassic feldspar from the potassic alteration assemblage in the Maria Cristina mine. Incremental heating experiments were carried out at the $^{40}\text{Ar}/^{39}\text{Ar}$ Geochronology Laboratory of the University of Geneva. Optically pure mineral separates were wrapped in aluminum foil packets and encapsulated along with neutron flux monitor packets (sanidine TCR) into sealed quartz vials, which were irradiated in the Oregon State University Triga reactor. Corrections for interfering reactions during irradiation are the following: $(^{40}\text{Ar}/^{39}\text{Ar})_{\text{K}} = 0.00086$; $(^{36}\text{Ar}/^{37}\text{Ar})_{\text{Ca}} = 0.000264$; and $(^{39}\text{Ar}/^{37}\text{Ar})_{\text{Ca}} = 0.000673$. The procedure for gas extraction, using a CO_2 laser, calculation of J values, and for the mass spectrometry are described in Singer and Pringle (1996). All ages were calculated using the decay constants of Steiger and Jäger (1977).

Results

Plateau ages were obtained for the two samples (Fig. 9). The incremental heating experiment performed on the amphibole sample gave a seven-step plateau containing 78.0 percent of the total ^{39}Ar released, yielding an age of 93.6 ± 0.4 Ma. These plateau steps define an inverse isochron age of 94.36 ± 1.08 Ma, with a $^{40}\text{Ar}/^{36}\text{Ar}$ intercept of 292.4 ± 4.1 . The experiment on the K feldspar sample yielded a 10-step

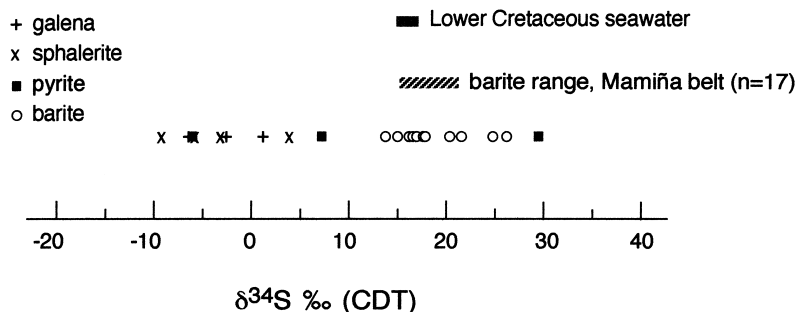


FIG. 8. Sulfur isotope composition of pyrite, sphalerite, galena, and barite from the Maria Cristina deposit, together with the $\delta^{34}\text{S}$ range of barite from the Mamiña belt (Lieben et al., 1996) and the Lower Cretaceous seawater $\delta^{34}\text{S}$ range (Claypool et al., 1980).

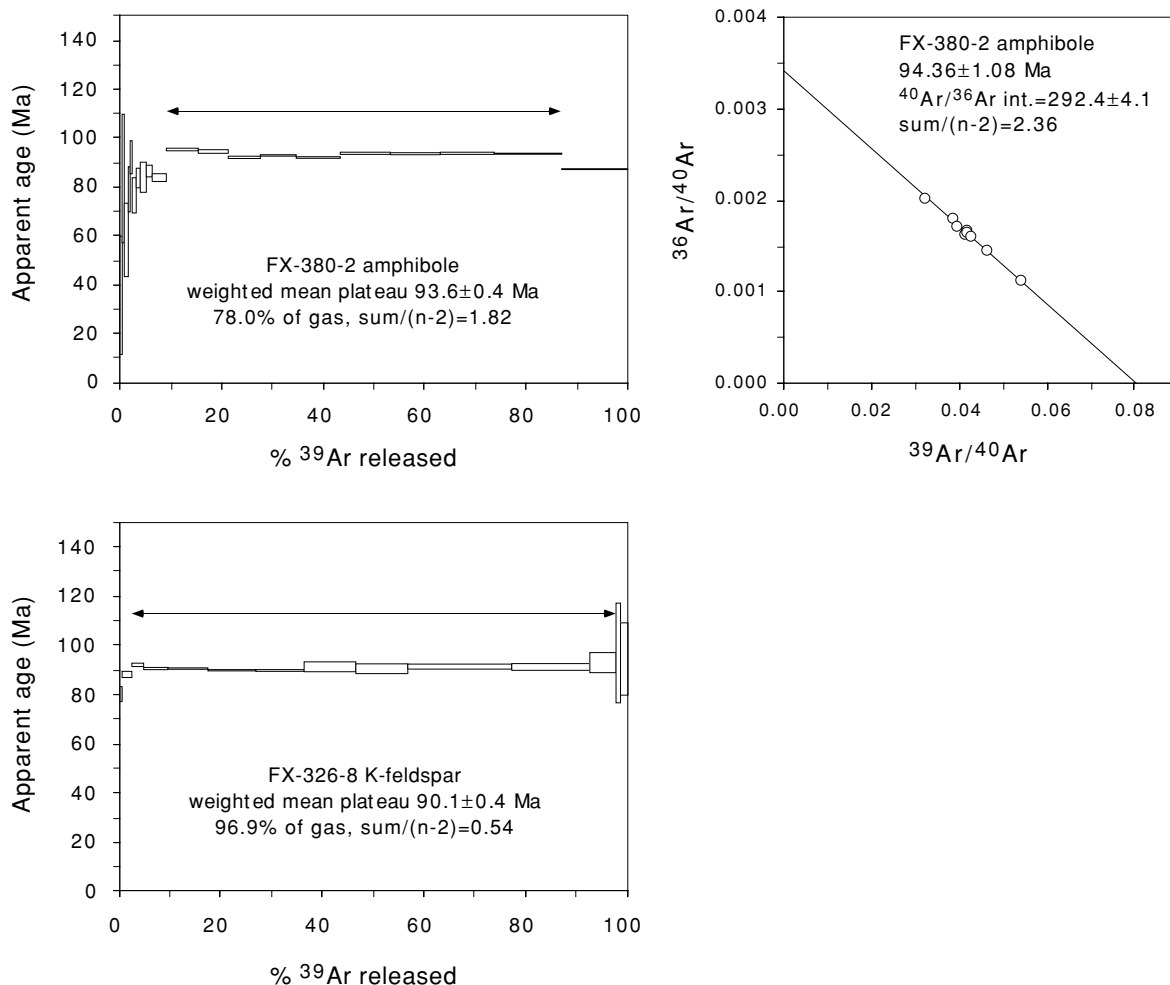


FIG. 9. $^{40}\text{Ar}/^{39}\text{Ar}$ incremental heating age spectra and inverse isochron diagram for samples FX-380-2 and FX-326-8, respectively, of hornblende of the diorite intrusive stock and K feldspar from the potassically altered porphyry at Maria Cristina.

plateau, containing 96.9 percent of the total ^{39}Ar released, which yielded an age of 90.1 ± 0.4 Ma. The limited spread in $^{40}\text{Ar}/^{39}\text{Ar}$ for this sample impedes a reliable inverse isochron age calculation. Only minor diffusional argon loss effects are shown for the lower temperature steps.

Interpretation

The hornblende data are interpreted as the emplacement age of the intrusion in view of the high-closure temperature of hornblende (McDougall and Harrison, 1988) and the high-level emplacement of the intrusion. The data indicate a Cenomanian age for the hornblende diorite intrusion, which is consistent with the geologic information (Abad, 1980) and may correspond to a late and main phase of emplacement of the mid-Cretaceous batholith (Farrar et al., 1970; Zentilli, 1974; Ménard, 1995; Dallmeyer et al., 1996). Although a more detailed study might reveal a more sequential emplacement of the dioritic intrusive bodies, this age is taken as broadly representative of the whole stock.

The age obtained for the K feldspar sample requires a more indepth discussion, in view of the lower closure temperature in the 150° to 200°C range of such a mineral (McDougall and

Harrison, 1988). The good plateau of this sample shows that it was not reheated significantly later than the time of the mid-Cretaceous intrusive activity. The K feldspar date gives a slightly younger age than the hornblende date outside the analytical error, according to the plateau ages. The K feldspar date may correspond to the age of porphyry intrusion and mineralization or to the age of a regional cooling and uplift that took place after the mineralization (e.g., Marschik et al., 1997). The available geologic information indicates a relationship between the porphyry and the mid-Cretaceous diorite intrusion, and suggests that the K feldspar age is either a cooling age related to the emplacement of the porphyry, or a slightly younger event than the porphyry. In this context, cooling from 450°C , the hornblende closure temperature, to 150° to 200°C , the K feldspar closure temperature, would probably last less than 1 m.y. In the first scenario, the data would indicate a 2 to 3 m.y. younger age for the porphyritic intrusion of Maria Cristina in comparison with the other part of the intrusion represented by the hornblende sample. In the second scenario, the data may indicate the end of the mid-Cretaceous thermal event and/or a regional uplift related to the onset of compressional deformation.

Conclusions

The geological and geochemical characteristics of the Maria Cristina deposit, including its epigenetic origin, the high-grade pyrite- and Ag-rich lead and zinc sulfide paragenesis, the occurrence of partly retrograde skarn minerals, and the $\delta^{34}\text{S}$ values of sulfides around 0 per mil, are those shared by the spectrum of deposits comprising the Zn-Pb skarn deposits of the western United States, northern Mexico, and Peru (Einaudi et al., 1981; Meinert, 1987; Megaw et al., 1988; Titley, 1993; Megaw, 1998). In this spectrum, the Maria Cristina deposit has a relatively proximal character by its occurrence at the contact of small potassically altered porphyritic intrusive bodies. The ore deposit is most likely related to the mid-Cretaceous intrusive activity and is controlled by faults. A main control for the sulfide ore formation might have been neutralization of acidic fluids as they migrated away from the intrusive center into the carbonate rocks. This ore style contrasts with that of the Mamiña belt barite deposits, which show no obvious spatial relationship to intrusive rocks and are in part more lithologically controlled, with characteristics similar to those of Mississippi Valley-type deposits.

This duality of Pb-Zn and Ba occurrence styles within the same mining camp is shown by other districts comprising high-temperature intrusion-related carbonate-replacement base metal deposits, such as the Colorado mineral belt (Beatty et al., 1990), and raises the unanswered question whether there can be a genetic relationship between Mississippi Valley-type and Zn-Pb skarn deposits in some particular cases or whether they are merely the result of a superposition of different metallogenic processes in time at the same location (Skinner, 1990). The question of a genetic link between the Maria Cristina deposit and the Mamiña belt cannot be fully addressed in the frame of this study. Support for this hypothesis can be gained from a more indepth dating and structural study and from the study of ore occurrences within this belt, presenting apparently similar characteristics as those of the Maria Cristina deposit. The similarity in lead isotope composition of the two different ore styles suggests a similar metal source. An additional element to this question is given by the strontium and sulfur isotope of the Maria Cristina barite, which suggests an interaction between magmatic and carbonate reservoirs and, therefore, supports a genetic association of the barite with the intrusion-related mineralizing process.

Acknowledgments

This study was supported by a National Swiss Foundation grant (20-47.260.96). The authors acknowledge L. Llinares, who made the sulfur isotope analyses at the Stable Isotope Laboratory of the University of Lausanne (J. Hunzicker, J. Spangenberg), and T. Ton-That and Y. Vincze who performed the $^{40}\text{Ar}/^{39}\text{Ar}$ incremental heating experiments, along with B. Singer for a rough interpretation of the data. This manuscript benefited from constructive comments by L. Meinert, W. Atkinson, and an anonymous reviewer.

REFERENCES

Abad, E., 1980, Cuadrángulos Estación Algarrobal, Yerbos Buenas, Cerro Blanco, Merceditas y Tres Morros, Región de Atacama: Instituto de Investigaciones Geológicas, Carta Geológica de Chile, v. 38, 48 p.

- Arévalo, C., and Grocott, J., 1997, The tectonic setting of the Chañarcillo Group and the Bandurrias Formation: An Early-Late Cretaceous sinistral transpressive belt between the Coastal Cordillera and the Precordillera, Atacama region, Chile: Congreso Geológico Chileno, 8th, Antofagasta Actas 3, p. 1604-1607.
- Beatty, D.W., Landis, G.P., and Thompson, T.B., eds., 1990, Carbonate-hosted sulfide deposits of the central Colorado mineral belt: ECONOMIC GEOLOGY MONOGRAPH 7, 424 p.
- Cisternas, M.E., and Díaz, L., 1990, Geologic evolution of the Atacama basin during the Lower Cretaceous, in Fontboté, L., Amstutz, G.C., Cardozo, M., Cedillo, E. and Frutos, J., eds., Stratabound ore deposits in the Andes: Berlin, Springer-Verlag, p. 495-504.
- Claypool, G.E., Holser, W.T., Kaplan, I.R., Sakai, Z., and Zak, I., 1980, The age curves of sulfur and oxygen isotopes in marine sulfate and their mutual interpretation: Chemical Geology, v. 28, p. 199-260.
- Coira, B., Davidson, J., Mpodozis, C., and Ramos, V., 1982, Tectonic and magmatic evolution of the Andes of northern Argentina and Chile: Earth Science Reviews, v. 18, p. 303-332.
- Dallmeyer, R.D., Brown, M., Grocott, J., Taylor, G.K., and Treloar, P.J., 1996, Mesozoic magmatic and tectonic events within the Andean plate boundary zone, 26°-27°30' S, north Chile: Constraints from $^{40}\text{Ar}/^{39}\text{Ar}$ mineral ages: Journal of Geology, v. 104, p. 19-40.
- Díaz, F., Bembo, M.S., Bravo, N., Gutierrez, A., Monti, S., Salinas, M., and Vogel, S., 1981, Mapa metalogénico pronóstico de la III Región: Santiago, Instituto de Investigaciones Geológicas, Unpublished report, 990 p.
- Díaz, L., 1990, The Mamiña barite mine, in Fontboté, L., Amstutz, G.C., Cardozo, M., Cedillo, E. and Frutos, J., eds., Stratabound ore deposits in the Andes: Berlin, Springer-Verlag, p. 523-536.
- Einaudi, M.T., and Burt, D.M., 1982, Introduction: Terminology, classification, and composition of skarn deposits: ECONOMIC GEOLOGY, v. 77, p. 745-754.
- Einaudi, M.T., Meinert, L.D., and Newberry, R.J., 1981, Skarn deposits: ECONOMIC GEOLOGY 75TH ANNIVERSARY VOLUME, p. 317-391.
- Farrar, E., Clark, A.H., Haynes, S.J., Quirt, S.G., Conn, H., and Zentilli, M., 1970, K-Ar evidence for the post Paleozoic migration of granitic intrusion foci in the Andes of northern Chile: Earth and Planetary Science Letters, v. 10, p. 60-66.
- Grocott, J., Brown, M., Dallmeyer, R.D., Taylor, G.K., and Treloar, P.J., 1994, Mechanisms of continental growth in extensional arcs: An example from the Andean plate-boundary zone: Geology, v. 22, p. 391-394.
- Jurgan, H., 1977, Strukturelle und lithofazielle Entwicklung des andinen Unterkreide Beckens im Norden Chiles (Provinz Atacama): Geotektonische Forschungen, v. 52, p. 1-138.
- Lieben, F., 2000, Carbonate-hosted Pb-Zn± Ag and Ba deposits in the Chañarcillo Group, northern Chile: Multiple fluid types and genetic processes: Terre & Environment, Genève, v. 22, 158 p.
- Lieben, F., Moritz, R., Fontboté, L., Fontignie, D., and Fallick, A., 1996, Ba and Pb-Zn occurrences in the Chañarcillo Group, northern Chile: Sr and S isotope constraints: Schweizerische Mineralogische und Petrographische Mitteilungen, v. 76, p. 265-275.
- Lieben, F., Moritz, R., Fontboté, L. and Chiaradia, M., 1999, Stratabound and vein-type Pb-Zn mineralization at Las Cañas, Chañarcillo Group, northern Chile: Fluid inclusion microthermometry, and sulfur and lead isotope constraints: Exploration and Mining Geology Journal v. 8, in press.
- Marschik, R., 1996, Cretaceous Cu (-Fe) mineralization in the Punta del Cobre belt, northern Chile: Université de Genève, Terre and Environment, v. 5, 200 p.
- Marschik, R., Chiaradia, M., and Fontboté, L., 1997a, Intrusion-related Cu (-Fe)-Au mineralization of the Punta del Cobre belt, Chile: Lead and sulfur isotopic constraints [abs.]: Biennial Society for Geology Applied to Mineral Deposits Meeting, 4th, Turku, Finland, Extended Abstract Volume, p. 655-658.
- Marschik, R., Singer, B.S., Munizaga, F., Tassinari, C., Moritz, R., and Fontboté, L., 1997b, Age of Cu (-Fe)-Au mineralization and thermal evolution of the Punta del Cobre district, Chile: Mineralium Deposita, v. 32, p. 531-546.
- McDougall, I., and Harrison, T.M., 1988, Geochronology and thermochronology by the $^{40}\text{Ar}/^{39}\text{Ar}$ method: New York, NY, Oxford University Press, 212 p.
- Megaw, P.K.M., 1998, Carbonate-hosted Pb-Zn-Ag-Cu-Au replacement deposits: An exploration perspective: Mineralogical Association of Canada Short Course Series, v. 26, p. 337-357.

- Megaw, P.K.M., Ruiz, J., and Titley, S.R., 1988, High-temperature, carbonate-hosted Ag-Pb-Zn (Cu) deposits of northern Mexico: *ECONOMIC GEOLOGY*, v. 83, p. 1856–1885.
- Meinert, L.D., 1987, Skarn zonation and fluid evolution in the Groundhog mine, Central mining district, New Mexico: *ECONOMIC GEOLOGY*, v. 82, p. 523–545.
- , 1992, Skarns and skarn deposits: *Geoscience Canada*, v. 19, p. 145–162.
- Ménard, J.J., 1995, Relationship between altered pyroxene diorite and the magnetite mineralisation in the Chilean iron belt, with emphasis on the El Algarrobo iron deposits (Atacama region, Chile): *Mineralium Deposita*, v. 30, p. 268–274.
- Mpodozis, C., and Ramos, V., 1989, The Andes of Chile and Argentina: Circum-Pacific Council for Energy and Mineral Resources, *Earth Science Series*, v. 11, p. 59–91.
- Ohmoto, H., and Rye, R.O., 1979, Isotopes of sulfur and carbon, in Barnes, H.L., ed., *Geochemistry of hydrothermal ore deposits*: New York, John Wiley, 2nd ed., p. 509–567.
- Puig, A., 1988, Geologic and metallogenic significance of the isotopic composition of lead in galenas of the Chilean Andes: *ECONOMIC GEOLOGY*, v. 83, p. 843–858.
- Ramdohr, P., 1980, *The ore minerals and their intergrowths*: Oxford, Pergamon, 1205 p.
- Rye, R.O., and Ohmoto, H., 1974, Sulfur and carbon isotopes and ore genesis: A review: *ECONOMIC GEOLOGY*, v. 69, p. 826–842.
- Schwarze, A., 1946, Informe de la mina Cristina: Santiago, Instituto de Investigaciones Geológicas, Unpublished report, 10 p.
- Segerstrom, K., 1968, Geología de las hojas Copiapó y Ojos del Salado: Instituto de Investigaciones Geológicas, *Carta Geológica de Chile*, v. 24, 58 p.
- Singer, B.S., and Pringle, M.S., 1996, Age and duration of the Matuyama-Brunhes geomagnetic polarity reversal from $^{40}\text{Ar}/^{39}\text{Ar}$ incremental-heating analyses of lavas: *Earth and Planetary Science Letters*, v. 139, p. 47–61.
- Skinner, B.J., 1990, A discussion of Sherman-type deposits: *ECONOMIC GEOLOGY MONOGRAPH* 7, p. 395–396.
- Spiro, B., and Puig, A., 1988, The source of sulfur in polymetallic deposits in the Cretaceous magmatic arc, Chilean Andes: *Journal of South American Earth Sciences*, v. 1, p. 261–266.
- Steiger, R.H., and Jäger, E., 1977, Subcommission on geochronology: Convention on the use of decay constants in geo- and cosmochronology: *Earth and Planetary Science Letters*, v. 139, p. 47–61.
- Tilling, R., 1976, El batolito Andino cerca de Copiapó, Provincia de Atacama: *Geología y petrología: Revista Geológica de Chile*, v. 3, p. 1–24.
- Titley, S.R., 1993, Characteristics of high-temperature, carbonate-hosted massive sulfide ores in the United States, Mexico and Peru: *Geological Society of Canada Special Paper*, v. 40, p. 585–614.
- Zentilli, M., 1974, Geological evolution and metallogenetic relationships in the Andes of northern Chile between 26° and 29° S: Unpublished Ph.D. thesis, Kingston, Ontario, Canada, Queen's University, 394 p.